# Electrophysiologically Detailed Models of the Right and Left Rabbit Atria: Pharmacological Impacts on Propagation and Arrhythmogenesis

OV Aslanidi, RS Dewey, AR Morgan, MR Boyett, H Zhang

University of Manchester, Manchester, UK

## Abstract

*Experimentally observed differences in the action potential (AP) properties – primarily, refractoriness – between the left (LA) and right (RA) atria are believed to be important in maintaining atrial fibrillation (AF). However, relationships between the underlying ionic differences in the LA and RA cells, as well as their impacts on the tissue refractoriness and susceptibility to AF are unknown. We quantify such relationships by developing detailed AP models for LA and RA, studying refractory and vulnerable properties of both tissues, and pharmacological impacts controlling them.*

## 1. Introduction

Reentrant excitation waves are widely associated with mechanisms of atrial fibrillation (AF), but the exact electrophysiological bases of initiation and maintenance of AF are still not fully understood [1, 2]. Experimental evidence points to a particularly important role of the left atrium (LA) in maintaining atrial fibrillation (AF). Animal models [3] and clinical studies [4] suggest the presence of LA "driver" regions as localized high-frequency reentrant sources for AF. LA refractoriness is shorter than right atrial (RA) [5], potentially explaining the preferential role of the LA reentry in AF. Despite the evidence for important electrophysiological differences between LA and RA, there are no detailed models describing them at either ionic, cell or tissue levels.

The aim of the present work is to identify ionic mechanisms of the left to right atrial AP differences and reconstruct single cell AP models for rabbit LA and RA. As our findings pointed to significant differences in the rapid delayed rectifier current ($I_{Kr}$) and the transient outward current ($I_{to}$) between LA and RA cells, we also evaluated the effect of the $I_{Kr}$ and $I_{to}$ blockers on electrophysiological differences between RA and LA tissue models – primarily, in tissue refractoriness, vulnerability to unidirectional conduction block and stability of reentry – thus, identifying potential ionic targets for the anti-arrhythmic drug action in the atria.

## 2. Methods

The dynamics of electrical processes in cardiac tissues are standardly described by the following equation [6, 7]:

$$\frac{\partial V}{\partial t} = \nabla \cdot \mathrm{D} \nabla V - \frac{I_{\mathrm{ion}}}{C_m}. \qquad (1)$$

Here $V$ (mV) is the membrane potential, $\nabla$ – a spatial gradient operator, $t$ – time (s), D – diffusion coefficient ($mm^2$ $ms^{-1}$) that characterizes electrotonic spread of voltage via gap junctional coupling, $I_{ion}$ – the total ionic current (pA), and $C_m$ (pF) – the membrane capacitance.

A biophysically detailed model describing individual membrane ionic currents comprising $I_{ion}$ for a rabbit atrial myocyte has been developed by Lindblad et al. [8]. It accurately reproduces the voltage-clamp data on which it has been based, and provides feasible morphologies of the rabbit atrial AP, but has some limitations: (i) it uses hybrid experimental datasets from cells in rabbit LA, the sinoatrial node and the ventricles; (ii) it ignores regional differences in the electrical properties of atrial cells. However, APs in rabbit LA and RA cells have different morphologies and rate-dependence [9, 10].

We develop a new family of AP models for rabbit LA and RA cells that (i) is based on experimental data obtained from rabbit atrial cells, and (ii) incorporates details of regional differences in cell electrical properties. First, the Lindblad et al. model [8] is modified in order to incorporate available experimental data [11-16] for the kinetics of major ionic currents from rabbit atrial cells (Fig. 1). Second, differences in ionic currents in between LA and RA cells are introduced (see below) based on experimental measurements [9, 10].

Eq. (1) is used to simulate AP propagation in the respective 1D and 2D atrial tissues. The diffusion coefficient is set to the value D = 5 $mm^2$ $ms^{-1}$, which produces the AP conduction velocity of ~0.5 m/s, as seen in experiments [17]. Eq. (1) is solved using the explicit Euler's method with the time and space steps $\Delta t = 0.005$ ms and $\Delta x = 0.1$ mm, respectively.

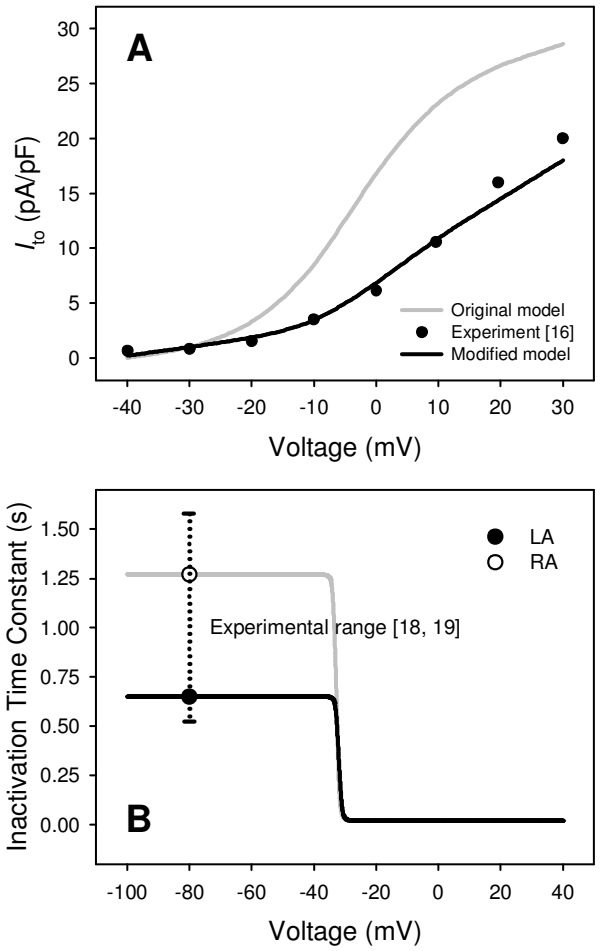


Fig. 1. Properties of the transient outward current, $I_{to}$, in rabbit atrial cells. A: current-voltage (I-V) relationships computed from the original model [8], our modified model and measured in experiments. Simulated I-V curves (solid lines) are plotted along with the respective experimental data (dots). B: fast inactivation time constants for $I_{to}$ in LA and RA are modeled as sigmoid curves connecting discrete values of fast inactivation times (60 ms) measured experimentally at +20 mV [16, 19], and fast reactivation times (symbols) measured at -80 mV [18, 19].

## 3. Results

Fig. 1A illustrates fitting ionic currents in LA and RA models to experimental data using the transient outward current, $I_{to}$, as an example. Similar techniques were used to model other currents: fast sodium, $I_{Na}$ [11], L-type calcium, $I_{CaL}$ [12, 13], slow and fast delayed rectifiers, $I_{Ks}$ and $I_{Kr}$ [9, 14], and outward rectifier, $I_{K1}$ [15].

Differences between the LA and RA were introduced based on experimental data obtained from dog [9] and rabbit [10]. Detailed studies of canine atrial cells [9] have shown insignificant differences in I-V relationships for $I_{CaL}$, $I_{Ks}$, $I_{K1}$ and $I_{to}$ between LA and RA cells. Reported small differences in the current density of $I_{Kr}$ – it is ~30% higher in LA than in RA – produced small differences in the AP duration when incorporated into the model. However, large variations of the AP morphologies have been reported between rabbit LA and RA [10]. The AP differences progressively increased as the pacing cycle length was increased from 500 to 2000 ms, but were almost completely eliminated by 4-AP, a selective blocker of the transient outward $K^+$ current, $I_{to}$.

Hence, as steady-state characteristics of $I_{to}$ do not vary between LA and RA [9], rate-dependent variations of AP morphologies between LA and RA [10] can be attributed to differences in the kinetics of $I_{to}$. Rate-dependence of $I_{to}$ is well-known [18, 19], and is determined by time constants of reactivation (recovery from inactivation) of this current. The fast time constants of reactivation in rabbit atrial cells vary in the range 500-1600 ms [18, 19].

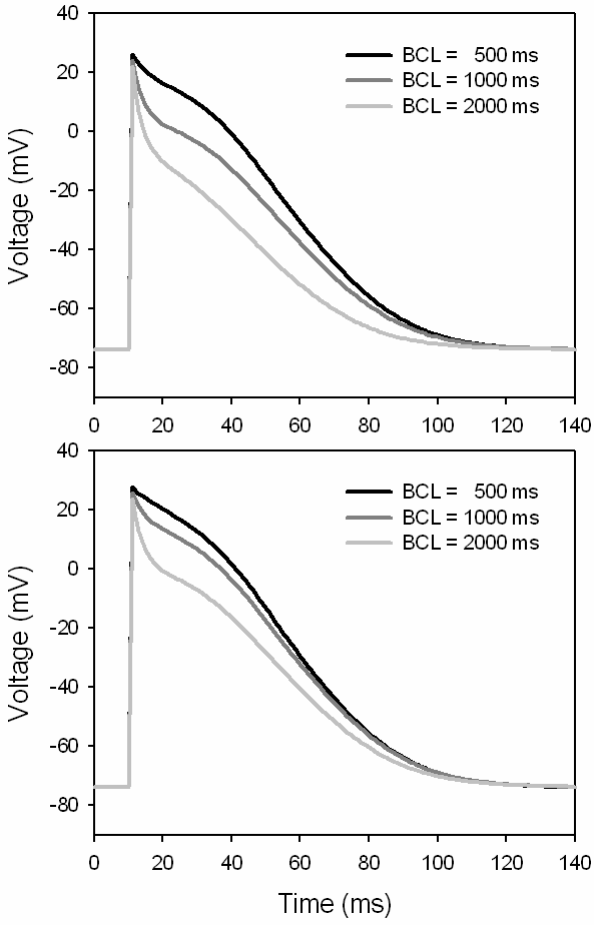


Fig. 2. Rate-dependence of APs simulated with the LA and RA cell models (top and bottom, respectively). AP morphologies match the respective experimental recordings [10].

Fig. 1B illustrates incorporation of the reactivation time constants into the model. Fast inactivation time constant measured at +20 mV was set to the value 60 ms in both LA and RA models [16, 19]. Fast reactivation time constant was set to the value 650 ms in LA, and 1250 ms in RA. Thus, major heterogeneity between LA and RA was assumed in the fast reactivation time constant. This was sufficient to reproduce remarkably different AP rate-dependence in LA and RA.

Fig. 3 shows APs simulated using the developed LA and RA models. AP morphologies and rate-dependence are in a very good agreement with experimental data [10]. In LA, both the AP duration and plateau are significantly decreased when the basic cycle length (BCL) is increased from 500 to 1000, and then 2000 ms – whereas responses to similar BCL changes in RA are much smaller. These differences are eliminated when $I_{to}$ in the models is completely blocked (not shown, AP morphologies in both atria in this case are similar to APs in control simulations

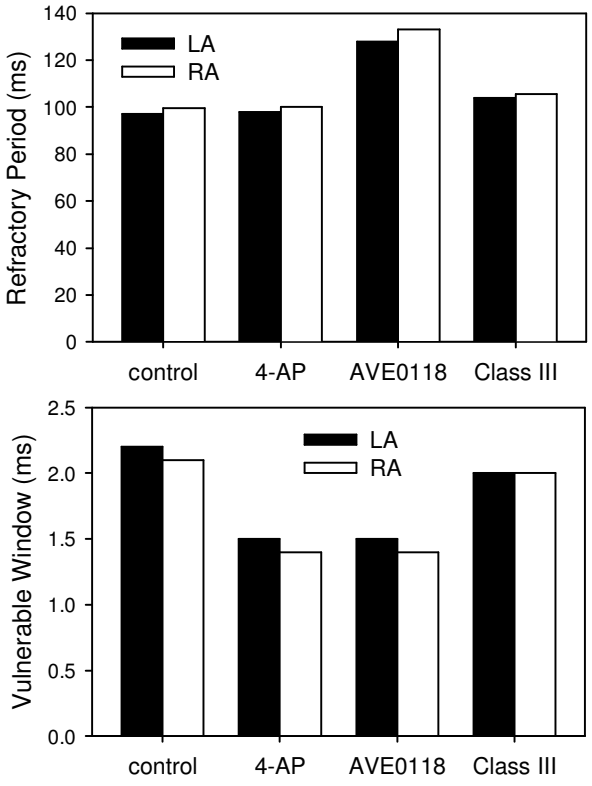


Fig. 3. Refractoriness and vulnerability of atrial tissues. Tissues were paced 5 times at BCL = 500 ms before the standard S1-S2 protocol [7] was applied in order to measure the vulnerable window of S2-pulse intervals resulting in unidirectional AP conduction block. RP was defined as the maximum S2 interval that failed to initiate AP conduction. The effect of AVE0118 was simulated by decreasing conductance of the background outward current $I_{sus}$ [8] by 50% in addition to 100% block of $I_{to}$. Class III drug effects were simulated by 100% block of $I_{Kr}$.

at BCL = 500 ms, but with slightly elevated plateaus), which reproduces experimentally observed effects of 4-AP, a selective $I_{to}$ blocker, in rabbit LA and RA [10].

AP propagation in 1D models of the LA and RA tissues was simulated in order to study effects of the atrial AP differences on refractoriness and vulnerability of the tissue. Fig. 3 shows refractory periods (RPs) and vulnerable windows measured in control simulations with the LA and RA tissues, as well as respective simulations of the effects of two $I_{to}$ blockers 4-AP and AVE0118, and a Class III drug dofetilide – a selective blocker of $I_{Kr}$. Note that AVE0118 blocks both the transient and sustained outward currents, $I_{to}$ and $I_{sus}$ [20], and has been used to stop AF by increasing refractoriness of atrial tissues. Our simulations show a greater increase of the RP with AVE0118 than with either 4-AP or dofetilide. The vulnerable window was also smallest with AVE0118 in comparison to other drugs. Hence, AVE0118 was not only more effective, but also relatively safe.

In order to illustrate a possible mechanism of the anti-arrhythmic drug action in the atria, we studied effects of dofetilide and AVE0118 on rotation of reentrant spirals waves in 30×30 $mm^2$ atrial tissues (Fig. 4). Reentry rotation in control was stable with periods of 118 and 122 ms in LA and RA. Dofetilide had little impact on stability of reentry – but application of AVE0118 resulted in its self-termination due to a substantial increase of the wavelength of the reentrant spiral wave (Fig. 4).

## 4. Discussion and conclusions

We have developed a new family of AP models for the LA and RA cells, which incorporates experimental data on atrial electrical properties [8-16]. Experimentally reported AP differences between LA and RA [10] were accounted for by different fast inactivation time constants of the transient outward current, $I_{to}$, in these two cell types. This provided a mechanistic explanation for different AP morphologies and rate-dependence between LA and RA. Note that similar approach has been used to simulate transmural AP heterogeneity in ventricles [7]. 1D models were used to study vulnerability of LA and RA tissues and evaluate pharmacological impacts controlling it. Blocking $I_{to}$ by 4-AP or AVE0118 enabled reduction of the vulnerable window, whereas additional effects of AVE0118 on $I_{sus}$ increased refractoriness of the tissue. Class III effects of dofetilite, a selective blocker of $I_{Kr}$, on the tissue refractoriness and vulnerability were significantly smaller. Besides, only AVE0118 allowed termination of reentry in atrial tissue. Hence, compared to Class III drugs that can increase vulnerable window [7], the atrial-specific drug AVE0118 [20] is both effective and relatively safe, and may provide a potential agent for pharmacological treatment of atrial arrhythmias.

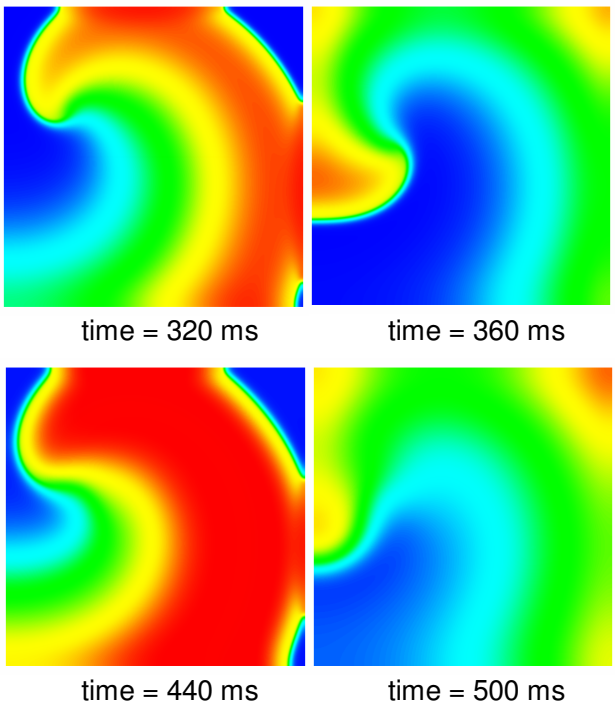


Fig. 4. Rotation of a reentrant spiral wave in LA tissue before (top) and after (bottom) AVE0118 application. In control, rotation of reentry is stable (before 400 ms), but after AVE0118 is applied wavelength of the spiral is increased (440 ms) and reentry is self-terminated (500 ms). Note that qualitatively similar behavior is observed in case of RA tissue.

## Acknowledgements

This research was supported by the BBSRC (UK).

## References

[1] Nattel S, Li D, Yue L. Basic mechanisms of atrial fibrillation - very new insights into very old ideas. Ann Rev Physiol 2000; 62: 51-77.

[2] Jalife J, Berenfeld O, Mansour M. Mother rotors and fibrillatory conduction: a mechanism of atrial fibrillation. Cardiovasc Res 2002; 54: 204-16.

[3] Harada A, Sasaki K, Fukushima T et al. Atrial activation during chronic atrial fibrillation in patients with isolated mitral valve disease. Ann Thorac Surg 1996; 61: 104-11.

[4] Mandapati R, Skanes A, Chen J, Berenfeld O, Jalife J. Stable microreentrant sources as a mechanism of atrial fibrillation in the isolated sheep heart. Circulation 2000; 101: 194-99.

[5] Sih HJ, Berbari EJ, Zipes DP. Epicardial maps of atrial fibrillation after linear ablation lesions. J Cardiovasc Electrophysiol 1997; 8: 1046-54.

[6] Qu ZL, Kil K, Xie FG, Garfinkel A, Weiss JN. Scroll wave dynamics in a three-dimensional cardiac tissue model: Roles of restitution, thickness, and fiber rotation. Biophys J 2000; 78: 2761-75.

[7] Benson AP, Aslanidi OV, Zhang H, Holden AV. The canine virtual ventricles: a platform for dissecting pharmacological effects on propagating and arrhythmogenesis. Prog Biophys Mol Biol 2008: 96: 187-208.

[8] Lindblad DS, Murphey CR, Clark JW, Giles WR. A model of the action potential and underlying membrane currents in a rabbit atrial cell. Am J Physiol 1996; 271: H1666-96.

[9] Li D, Zhang L, Kneller J, Nattel S. Potential ionic mechanism for repolarization differences between canine right and left atrium. Circ Res 2001; 88: 1168-75.

[10] Qi A, Yeung JA, Xiao J, Kerr CR. Regional differences in rabbit atrial repolarization: importance of transient outward current. Am J Physiol 1994; 266: H643-49.

[11] Gilliam FR, Starmer CF, Grant AO. Blockade of rabbit atrial sodium channels by lidocaine. Characterization of continuous and frequency-dependent blocking. Circ Res 1989; 65: 723-39.

[12] Ko JH, Park WS, Kim SJ, Earm YE. Slowing the inactivation of voltage-dependent sodium channels by staurosporine, the protein kinase C inhibitor, in rabbit atrial myocytes. Eur J Pharmacol 2006; 534: 48-54.

[13] Fedida D, Shimoni Y, Giles WR. Alpha-adrenergic modulation of the transient outward current in rabbit atrial myocytes. J Physiol 1990; 423: 257-77.

[14] Muraki K, Imaizumi Y, Watanabe M, Habuchi Y, Giles WR. Delayed rectifier $K^+$ current in rabbit atrial myocytes. Am J Physiol 1995; 269: H524-32.

[15] Ishii Y, Muraki K, Kurihara A, Imaizumi Y, Watanabe M. Effects of sematilide, a novel class III antiarrhythmic agent, on membrane currents in rabbit atrial myocytes. Eur J Pharmacol 1997; 331: 295-302.

[16] Wang Z, Feng J, Shi H, Pond A, Nerbonne JM, Nattel S. Potential molecular basis of different physiological properties of the transient outward $K^+$ current in rabbit and human atrial myocytes. Circ Res 1999; 84: 551-61.

[17] de Groot JR, Veenstra T, Verkerk AO et al. Conduction slowing by the gap junctional uncoupler carbenoxolone. Cardiovasc Res 2003; 60: 288-97.

[18] Fermini B, Wang Z, Duan D, Nattel S. Differences in rate dependence of transient outward current in rabbit and human atrium. Am J Physiol 1992; 263: H1747-54.

[19] Uese K, Hagiwara N, Miyawaki T, Kasanuki H. Properties of the transient outward current in rabbit sino-atrial node cells. J Mol Cell Cardiol 1999; 31: 1975-84.

[20] de Haan S, Greiser M, Harks E et al. AVE0118, blocker of the transient outward current $I_{to}$ and ultrarapid delayed rectifier current $I_{Kur}$, fully restores atrial contractility after cardioversion of atrial fibrillation in the goat. Circulation 2006; 114: 1234-42.

**Address for correspondence**

Oleg Aslanidi, Ph.D.

School of Physics and Astronomy
University of Manchester
Manchester M13 9PL
United Kingdom

oleg.aslanidi@manchester.ac.uk